ISSN 0023-1584, Kinetics and Catalysis, 2012, Vol. 53, No. 3, pp. 395–403. © Pleiades Publishing, Ltd., 2012.

Catalytic Behaviour of Gallium-Containing Mesoporous Silicas (MCM-41) in the Acetylation Reaction[1]

K. Bachari and R. M. Guerroudj

Centre de Recherche Scientifique et Technique en Analysesphysico–Chimiques (C.R.A.P.C) BP 248, Alger RP, Alger, 16004 Algerie

e-mail: bachari2000@yahoo.fr

Received May 9, 2011

Abstract—Liquid phase acetylation of 1,2-dimethoxybenzene with acetic anhydride has been examined for a series of acid gallium-mesoporous materials (MCM-41) with different Si/Ga ratios (Si/Ga = 80, 50 and 10) synthesized by microwave irradiation method. Physical adsorption of nitrogen, inductively coupled plasma, and the X-ray diffraction techniques, transmission electron microscopy, Fourier transform infrared spectroscopy, and a temperature-programmed desorption of pyridine were applied to characterize the catalysts. A mesoporous sample with Si/Ga = 10 showed better performance in the acid-cataiyzed acetylation of 1,2-dimethoxybenzene with acetic anhydride as an acylating agent. In addition, the kinetics of the reaction in the presence of these catalysts has been investigated.

DOI: 10.1134/S0023158412030032

The microwave–hydrothermal synthesis of molecular sieves is a relatively new area of research [1–7], The major advances of using microwaves for the synthesis are rapid attainment of crystallization temperature, volumetric heating leading to homogeneous nucleation, fast supersaturation caused by the rapid dissolution of precipitated gels and a reduced crystallization time [1–7], This technique is also energy efficient and economically reasonable [1–7]. On the other hand, Friedel–Crafts acetylation of aromatic compounds and aromatic heterocyclic compounds is an excellent example of electrophilic substitution catalyzed by acidic or basic catalysts, which has been widely used in the industry for the production of valuable organic intermediates. Preparation of aromatic ketones has received much attention in recent years because they are important intermediates in the synthesis of pharmaceuticals (naproxen, dextromethorphan, and ibuprofen), dyes, fragrances, and agrochemicals [8]. Conventionally, these reactions are carried out in presence of homogeneous catalysts such as $AlCl_3$, and BF_3, strong mineral acids like H_2SO_4, HF, or supported Lewis acid catalysts, using acid chloride or anhydride as an acylation agent [9].

Regrettably, the use of the above catalysts in the industry causes a lot of environmentally related problems as these solids are highly corrosive in nature and cannot be regenerated for recycling. Moreover, the separation of the homogeneous catalysts from the product mixture is difficult. Not infrequently Lewis acid catalysts form a complex with the product ketones, and to destroy the complex in the hydrolysis step to isolate product, a stoichiometric excess of the catalysts is needed. To avoid the above environmentally associated problems, it is desirable to develop a catalyst process which is stable, environmentally friendly, and recyclable. Novel solid catalytic systems that can mitigate the corrosion and environmental problems include the acid zeolites and zeolite–like molecular sieves, which are highly efficient, sustainable, recyclable, and ecologically friendly. Indeed, the acetylation of anisole and 1,2-dimethoxybenzene leads to the synthesis of *p*-acetylanisole and 4-acetylveratrole, commercially important products used as the precursors of a sun protector and of a component in the insecticide formulation [10], respectively. Various catalysts such as zeolites [11–14], heteropolyacids [15, 16], sulphated metal oxides [17] and A1SBA-15 [18] have been investigated in the Friedel–Crafts alkylation and acetylation reactions. The present study is focused on the liquid phase acetylation of 1,2-dimethoxybenzene with acetic anhydride over Ga–MCM-41 catalysts synthesized by the microwave radiation.

EXPERIMENTAL

Synthesis of the Catalysts

Microwave–hydrothermal (M-H) synthesis of mesoporous molecular sieves with Si/Ga ratios of 80, 50 and 10 (Ga–MCM-41) was performed using a MARS5 (CEM Corp., USA) microwave digestion system. This system operates at a maximum power of 1200 W, the power can be varied from 0 to 100% and is controlled by both pressure and temperature with the

[1] The article is published in the original.

highest values of 2456 kPa and 513 K, respectively. A 2.45 GHz microwave frequency was used which is the same as that implied in household microwave ovens.

The syntheses were carried out in double–walled digestion vessels with an inner liner and cover made up of Teflon PFA and an outer strength vessel shell of Ultem polyetherimide. In a typical synthesis, 21.32 g of sodium metasilicate ($Na_2SiO_3 \cdot 9H_2O$, "CDH") was dissolved in 60 g of water. The reaction mixture was stirred for 2 h. Meanwhile, cetyltrimethylammonium bromide (5.47 g, "OTTO Chemie") and gallium nitrate ($Ga(NO_3)_3 \cdot 8H_2O$, "Aldrich") were dissolved in 20 g of distilled water. Then, the resultant solution was added dropwise to the sodium metasilicate solution. The final mixture was stirred for 1 h. The pH of the gel was adjusted by using 2 M sulfuric acid (H_2SO_4, 98%, "Merck") and the gel was stirred for another 3 h. Thus obtained gel was allowed to crystallize under microwave-hydrothennal conditions at 373 K for for 2 h. The crystallized product was filtered off, washed with warm distilled water, dried at 383 K and finally calcined at 813 K in air for 6 h.

Characterization Techniques

The X-ray diffraction (XRD) patterns of samples were recorded with a powder XRD instrument (Rigaku D/Max 2500PC, Japan) operated at 40 kV and 50 mA using CuK_α radiation ($\lambda = 0.15418$ nm). The samples were scanned at a rate of 0.02° per step, and a scan speed of 17 min over the $1° \le 2\theta \le 10°$ range was used.

Fourier transform infrared spectra (FT-IR) in the effective range from 400 to 4000 cm^{-1} were recorded on a Nexus FT-IR 470 spectrometer (Nicolet Corp., USA) with KBr pellets.

The BET surface area and pore dimensions were determined using a NOVA 2000e analytical system made by "Quantachrome Corp." (USA). Pore size distribution and pore volume were calculated by Barrett–Joyner–Halenda (BJH) method. Morphology of the samples was inspected using transmission electron microscopy (TEM) with a Philips TEMCNAI-12 (100–120 kV accelerating voltage).

The gallium content in the samples was determined by inductively coupled plasma (ICP) technique (Vista-MAX, Varian).

The density and strength of the acid sites of the different Ga–MCM-41 samples were determined by the temperature-programmed desorption (TPD) of pyridine. A catalyst sample (ca. 100 mg) was evacuated for 3 h at 523 K and $P < 10^{-5}$ kPa, cooled then to ambient temperature in a flow of dry nitrogen and exposed to a stream of pyridine in nitrogen for 30 min. Finally, the physically sorbed pyridine was removed by heating the sample to 393 K for 2 h in a nitrogen flow. TPD of pyridine was performed by heating the sample in a nitrogen flow (50 mL/min) from 393 to 873 K with a rate of 10 K/min using a high-resolution thermogravimetric analyzer coupled with a mass spectrometer (SETARAM setsys 16MS). The observed weight loss was used to quantify the number of acid sites assuming that each mole of pyridine adsorbs a mole of protons.

Catalytic Testing

Acetylation of 1,2-dimethoxybenzene with acetic anhydride has been carried out under liquid phase conditions. The liquid phase reactor consists of two-necked 50 mL round bottom flasks duly fitted with a condenser in one end for cooling and another vent is closed with Teflon septum for collecting samples by glass syringe at regular intervals. The whole system was kept in a thermostated oil bath attached with a magnetic stirrer coupled with a heating plate. In a typical reaction, the catalyst was added to a solution containing 2.6 g 1,2-dimethoxybenzene (18.9 mmol), 0.4 g acetic anhydride (3.8 mmol) and 50 ml chlorobenzene together with 1 g nitrobenzene as internal standard. Then, the reaction mixture was heated to the required temperature and the samples were taken in regular time intervals. The collected samples were analyzed periodically by a gas chromatograph (HP-6890) equipped with a FID detector using a DB-5 capillary column. GC–MS (HP-5973) analysis confirmed the product composition followed from the gas chromatographic measurements.

RESULTS AND DISCUSSION

Characterization of the Samples

The small angle X-ray diffraction patterns of Ga–MCM-41 (Si/Ga = 80, 50, 10) synthesized by microwave irradiation method are shown in Fig. 1. The Ga–MCM-41(80) sample is characterized by a very strong (100) peak followed by (110) and (200) peaks of lower intensity. All three distinct Bragg reflections at low angles were indexed to a hexagonal lattice. However, when the gallium content increases (as Si/Ga ratio decreases from 50 to 10), reduced intensities of the long range ordered peaks were observed. However, compared with the patterns of the typical MCM-41 mesoporous molecular sieve acquired for both as-synthesized and calcined samples [19], the d_{100} spacing for Ga–MCM-41 samples is significantly larger than that for MCM-41 indicating the incorporation of Ga in the MCM-41 structure. The gallium content in Ga–MCM-41 is increased when Ga content in the reaction gel is increased (Table 1).

The porosity of the samples was evaluated making use of N_2 adsorption isotherms. The specific surface area, pore size distribution, and pore volume calculated by BET and BJH methods are summarized in Table 1. Figure 2 shows the adsorptionde–desorption isotherms of N_2 for three calcined samples Ga–MCM-41. The samples Ga–MCM-41 (80) and Ga–MCM-41 (50) exhibit conventional type IV isotherms with hysteresis loops caused by capillary con-

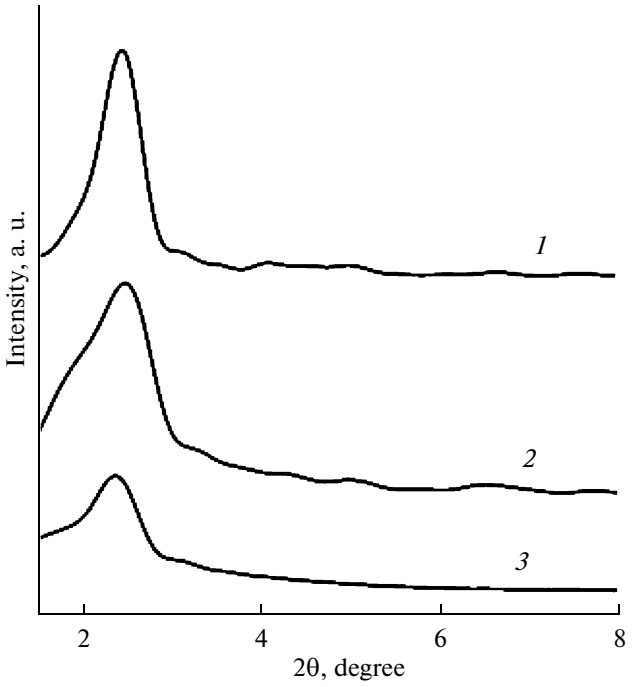

Fig. 1. XRD patterns of Ga–MCM-41 materials in the $1° \le 2\theta \le 10°$ range prepared by M-H process: Ga–MCM-41(80) (*1*), Ga–MCM-41(50) (*2*), and Ga–MCM-41(10) (*3*).

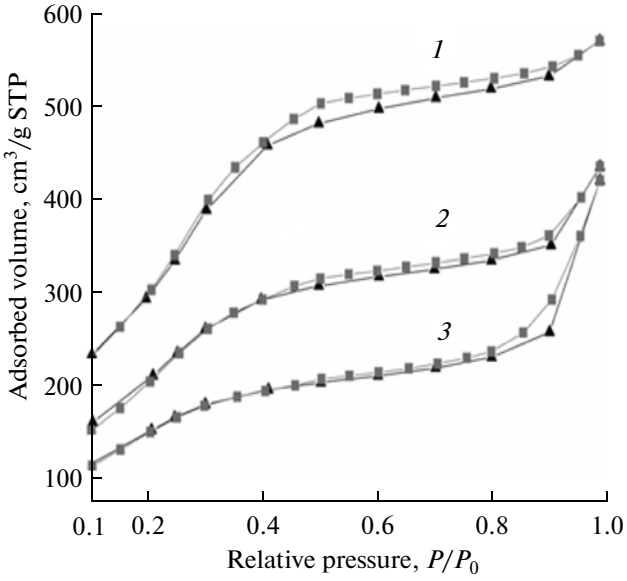

Fig. 2. N_2 physical adsorption-desorption isotherms of Ga–MCM-41 materials prepared by M-H process Ga–MCM-41(80) (*1*), Ga–MCM-41(50) (*2*), and Ga–MCM-41(10) (*3*).

densation in mesopores. It can be thus inferred that these two samples possess a pronounced mesoporous structure [19]. For these two samples one can identify three well-defined steps on the isotherms. A first step at relative pressures (P/P_0) of ca. 0.3–0.4 is characteristic of capillary condensation of uniform mesoporous materials, showing that the two samples have a uniform pore size distribution and a large pore volume. The region of isotherms corresponding to $P/P_0 < 0.3$ is due to a monolayer adsorption of nitrogen on the walls of the mesopore. The near horizontal section beyond $P/P_0 > 0.4$ represents the multilayer adsorption on the outer surface of the particles. In addition, from Fig. 2, it is evident that the isotherms of the sample Ga–MCM-41 (80) have a steep capillary condensation step at the same P/P_0, illustrating that this sample has a more uniform pore size distribution compared to other samples. Isotherms of the sample Ga–MCM-41 (10) can not be described by a typical type IV isotherm; this is attributed to the partial degradation of the mesoporous structure caused by incorporation of excess gallium into the MCM–41 mesoporous molecular sieve. However, based on the value of the specific surface area (690 m^2/g) listed in Table 1 and the XRD data (Fig. 1), the mesoporous structure partly persists in the sample Ga–MCM-41(10) but the long–ranged order is damaged.

Figure 3 presents the pore-size distribution curves for three calcined samples Ga–MCM-41 synthesized by the microwave irradiation method. For the samples Ga–MCM-41 (80) and Ga–MCM-41 (50) a narrow peak can be observed over the pore size range between 2 and 3 nm, and the intensity of the peak is high compared with that traced for the sample Ga–MCM-41(10). Accordingly, a uniform pore size distribution can be accepted for two Ga–MCM-41 samples. As the gallium content in the sample increases, the intensity of the peak on the pore size distribution curve decreases. It appears that an increased amount of gallium ions incorporated into the silica framework of MCM-41 mesoporous molecular sieve causes the partial degradation of the mesoporous framework, resulting in an irregular pore size distribution and a poor mesoporous

Table 1. Physico-chemical properties of different Ga–MCM-41(M-H) samples

Sample	Chemical analysis		S_{BET}, $m^2\ g^{-1}$	Pore volume, $cm^3\ g^{-1}$	Pore diameter, nm
	Si/Ga (gel)	Si/Ga			
Ga–MCM-41	10	9.8	690	0.66	3.0
Ga–MCM-41	50	48.9	947	0.88	2.8
Ga–MCM-41	80	79.4	1135	0.98	2.6

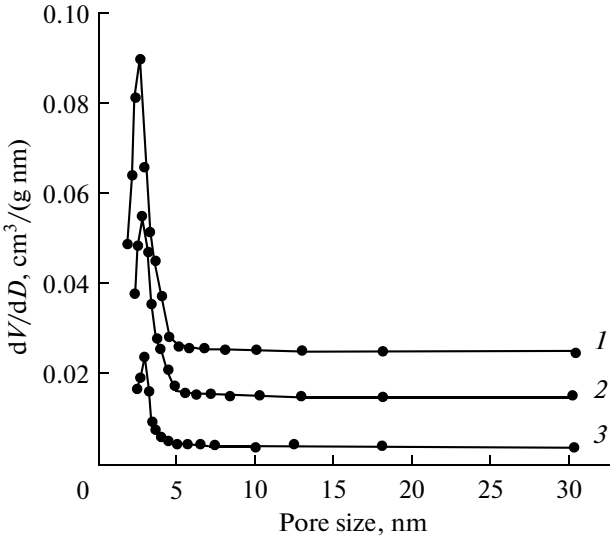

Fig. 3. Pore size distribution curves of the of Ga–MCM-41 materials prepared by M-H process: Ga–MCM-41(80) (*1*), Ga–MCM-41(50) (*2*), and Ga–MCM-41(10) (*3*).

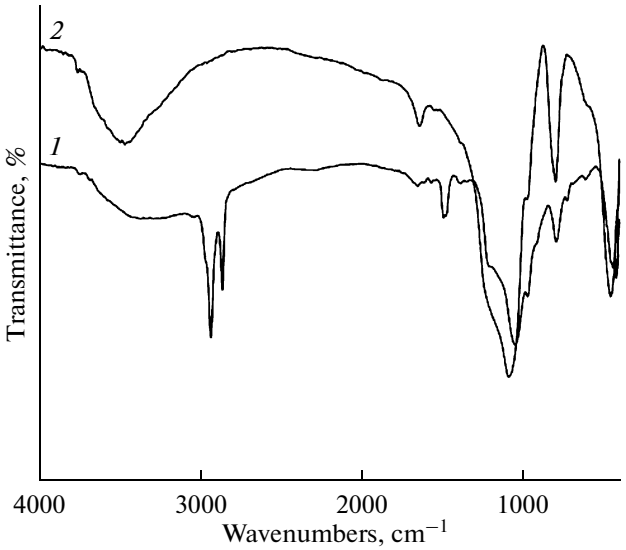

Fig. 4. FT-IR spectra of the Ga–MCM-41(50) material prepared by M-H process: before (*1*) and after calcinations (*2*).

ordering. From Table 1, it can be suggested that the specific surface area and pore volume of the Ga–MCM-41 samples gradually decrease with the increasing gallium content, most of the pores being 2.5–2.9 nm in radius. Combined with the results of XRD and N_2 adsorption isotherms, it is reasonable to conclude that the mesoporous ordering of the sample Ga–MCM-41 synthesized by microwave irradiation method gradually decreases as the content of gallium incorporated into the mesoporous framework increases.

Figure 4 presents the FT-IR spectra of the synthesized Ga–MCM-41 (50) sample before and after calcination at 813 K in air for 6 h. As shown in the figure, the band at 3500 cm^{-1} is related to water adsorbed on the surface of the catalyst. The bands at 1620–1640 cm^{-1} are caused by bending vibrations of the OH bonds [20]. The band at 1080 cm^{-1} is assigned to the asymmetric Si–O–Si stretching modes. The band around 810 cm^{-1} is attributed to the corresponding symmetric vibration of Si–O–Si bonds, while the band at 460 cm^{-1} is assigned to deformation vibrations of the Si–O–Si bonds. The bands at 2921, 2850 and 1480 cm^{-1} are the characteristic bands of the surfactant alkyl chains. After the sample Ga–MCM-41 (50) was calcined at 813 K in air for 6 h, the bands at 2921, 2850 and 1480 cm^{-1} disappeared, indicating that the template had been effectively removed. The TBM images of the samples Ga–MCM-41 (80) and Ga–MCM-41(50) are shown in Fig. 5. It appears that these two samples exhibit arrays assembled into hexagonal patterns, indicating that these two samples synthesized under microwave irradiation conditions have a mesoporous framework. However, the mesoporous ordering of the sample Ga–MCM-41 (50) is poor compared with that of the sample Ga–MCM-41 (80). Moreover, gallium species doesn't occur on the surface of these two samples as the particles and/or clusters as evidenced by the inspection of TEM images in Fig. 5.

TPD of pyridine was used to assess the acid site distribution and amounts of acid sites in the Ga–MCM-41 samples synthesized under microwave irradiation condition with the data collected in Table 2. The presence of acid sites with weak (423 and 633 K), moderate (633–743 K) and strong (> 743 K) acidity was found in all samples. Whereas weak acid sites are attributed to surface hydroxyl groups, medium and strong acidity can be associated also with non-framework Ga_2O_3 and/or mixed Ga–Si oxide particles which can appear as a result of a partial structural collapse of Ga–MCM-41 caused by incorporation of gallium atoms into the walls of MCM-41 frameworks. It should be noted that the total number of acid sites with medium and strong acidity in the Ga–MCM-41(10) sample prepared by M-H synthesis is higher than that of Ga–MCM-41(50) and Ga–MCM-41 (80).

Catalytic Activity

Catalytic performances of Ga–MCM-41 (M-H) materials with different Si/Ga ratio in the acetylation of 1,2-dimethoxybenzene with acetic anhydride. The acetylation of 1,2-dimethoxybenzene (1,2-DMB) with acetic anhydride conventionally produces acetic acid. However in our experiments 3,4-dimethoxyacetophenone was the only product of the acetylation. A probable reason is that both *ortho*-positions of 1,2-DMB are sterically hindered for the electrophilic reaction, and acetylation preferentially occurs at the fourth position which is the most preferred since it is

in *para*-position to one of the methoxy substituents. Accordingly, no products other than 3,4-dimethoxyacetophenone were found in the product mixture.

The conversion and selectivity in the acetylation of 1,2-DMB over Ga–MCM-41 (M-H) catalysts with different Si/Ga ratio (Si/Ga = 80, 50, and 10) at a reaction temperature of 333 K and under standard reaction conditions are given in Table 3. The sequence of catalytic activity is: Ga–MCM-41 (M-H)(10) > Ga–MCM-41 (M-H)(50) > Ga–MCM-41 (M-H)(80). It can be seen that the Ga–MCM-41 (10) catalyst is the most efficient catalyst that shows a much higher conversion of acetic anhydride than other catalysts studied. When reacted for 95 min, acetic anhydride was fully converted with 100% selectivity to 3,4-dimethoxyacetophenone over the Ga–MCM-41 (10) catalyst. A very high level of activity of Ga–MCM-41 (10) compared to other Ga–MCM-41 (M-H) catalysts can be rationalized in terms of higher acidity of this catalyst (Table 2). On the other hand, a lower activity of Ga–MCM-41(M-H)(80) which has the highest surface area and largest pore volume can be explained by the presence of lower number of active sites on the porous surface. It is instructive to compare the catalysts described in the present work with zeolites catalysts investigated earlier under similar conditions. The order of decreasing activity for the catalysts is: Ga–MCM-41(M-H)(10) > BEA > MFI. Note that although the acidity of the zeolites catalysts is much higher than that of the Ga–MCM-41(M-H)(10), the catalytic activity of the mesoporous catalyst is superior to that of the zeolite based catalysts. Thus, it can be concluded that the accessibility of the active sites to the reactant molecules is higher in Ga–MCM-41(M-H)(10) than that in the zeolite catalysts. Favourable access is facilitated by vary high specific surface areas, significant pore volume, and well–developed regular pore structure composed by large pores. These exceptional textural characteristics of the Ga–MCM-41(M-H)(10) account for its higher catalytic activity and the results outlined above provide an additional evidence that a high surface area and large pores are the important prerequisites for the development of catalysts active in the acetylation of substituted aromatic compounds. As the Ga–MCM-41(M-H)(10) catalyst was found to be highly active, this system was chosen to investigate the effect of other reaction parameters such as the reaction temperature, the stoichiometric ratio 1,2-DMB/AC, weight of the catalysts and the recycling ability of the

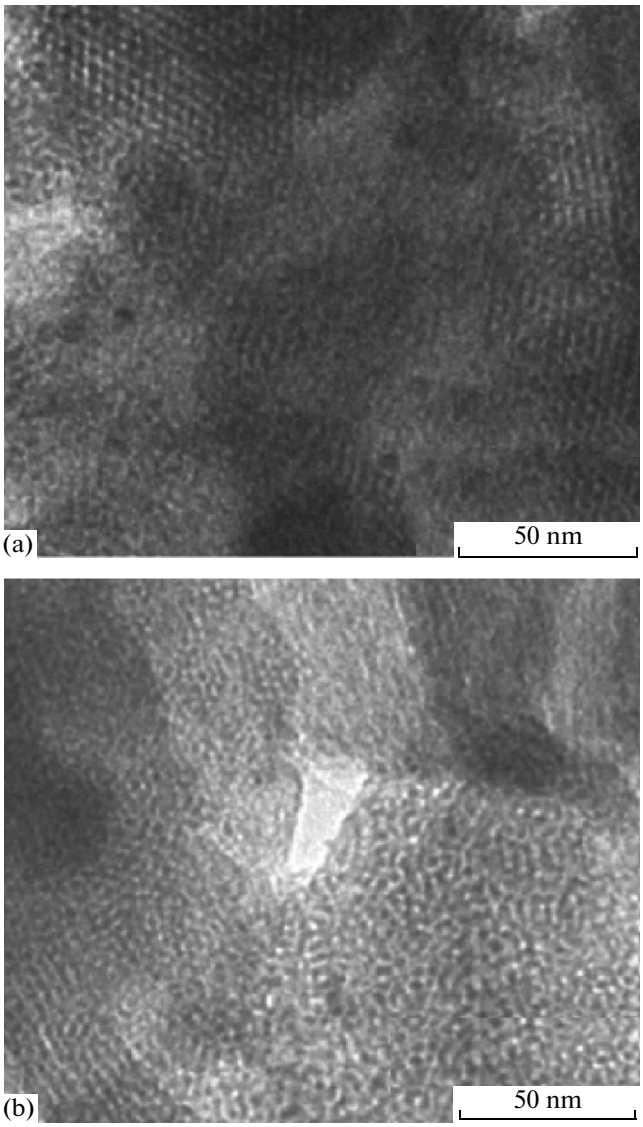

Fig. 5. TEM images of the Ga–MCM-41(80) (a) and Ga–MCM-41(50) (b) materials prepared by M-H process.

Table 2. Density and strength of acid sites of Ga–MCM-41(M-H) catalysts with different Si/Ga ratios (Si/Ga = 80, 50, 10)

Sample	Acid sites, mmol/g			
	weak (423–633 K)	medium (633–743 K)	strohg (>743 K)	total (medium and strong acid sites)
Ga–MCM-41(10)	0.539	0.191	0.224	0.415
Ga–MCM-41(50)	0.601	0.123	0.179	0.302
Ga–MCM-41(80)	0.748	0.107	0.145	0.252

Table 3. The conversion and selectivity of 1,2-dimethoxybenzene over Ga–MCM-41(M-H) catalysts with different Si/Ga ratio (Si/Ga = 80, 50, and 10)

Sample	Acetic anhydride conversion (%)	Selectivity to 3,4-dimethoxyacetophenone (%)
Ga–MCM-41(10)	100.0	100.0
Ga–MCM-41(50)	88.3	100.0
Ga–MCM-41(80)	66.5	100.0

Note: A reaction temperature of 333 K, stoichiometric ratio 1,2-DMB/AC = 5, catalyst weight of 0.1 g and a reaction time of 2 h.

Table 4. Catalytic activities of Ga–MCM-41(M-H)(10) at different temperatures: 313, 333 and 353 K

Temperature, K	Time*, min	Selectivity to 3,4-dimethoxyacetophenone, %	Apparent rate constant k_a, 10^3 min^{-1}
313	210.0	100.0	13.2
333	95.0	100.0	40.3
353	40.1	100.0	94.4

Note: Stoichiometric ratio 1,2-DMB/AC = 5, catalyst weight of 0.1 g. * Time required for complete conversion of acetic anhydride.

catalysts on conversion of acetic anhydride and selectivity in the acetylation of 1,2-DMB.

The effect of reaction temperature on the acetylation of 1,2-dimethoxybenzene with acetic anhydride. The effect of reaction temperature on conversion of acetic anhydride in the acetylation of 1,2-DMB over Ga–MCM-41(M-H)(10) at different reaction time lengths is shown in Table 4. Conversion of acetic anhydride increases with increasing reaction temperature. However, selectivity to 3,4-dimethoxyacetophenone was about 100% for all the reaction temperatures studied. Note that the rate of the reaction at lower temperature is relatively low. On the other hand, at the reaction temperature above 333 K, the rate of the reaction is very high. The apparent rate constant of the reaction at different reaction temperature was calculated using the pseudo-first order rate law:

$$\log(1/1 - x) = (k_a/2.303)(t - t_0),$$

where k_a is the apparent first-order rate constant, x is the fractional conversion of acetic anhydride, t is the reaction time and t_0 is the induction period corresponding to the time required to reach an equilibrium temperature. A plot of $\log(1/1 - x)$ as a function of time gives a linear plot over a wide range of acetic anhydride conversions (Fig. 6). As expected, the apparent rate constant for the acetylation reaction increased from 13.2×10^{-3} min^{-1} to 94.4×10^{-3} min^{-1} as the reaction temperature was increased from 313 to 363 K. The activation energy for the Ga–MCM-41(10) calculated from an Arrhenius plot can be estimated as 27.6 kJ mol^{-1}. From these results, it was found that the reaction temperature of 333 K is the best temperature for Ga–MCM-41 (10) and is a preferred temperature for catalytic studies described below.

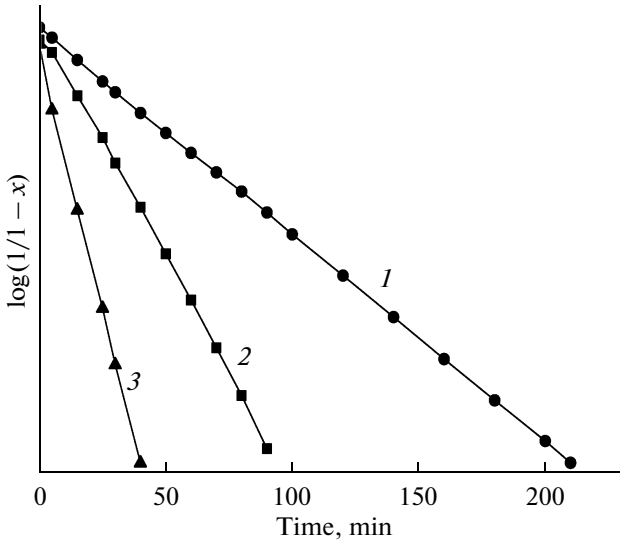

Fig. 6. The plot of $\log(1/1 - x)$ as a function of reaction time of Ga–MCM-41(M-H)(10) catalyst at different temperatures: 313 (*1*), 333 (*2*) and 353 K (*3*). Stoichiometric ratio 1,2-DMB/AC = 5, catalyst weight of 0.1 g.

The effect of the stoichiometric ratio 1,2-DMB/AC on the acetylation of 1,2-dimcthoxybenzcne with acetic anhydride. The effect of the stoichiometric ratio 1,2-DMB/AC on the reaction rate constant of acetic anhydride was studied over Ga–MCM-41(M-H)(10) at

Table 5. The conversion and the selectivity in the acetylation of 1,2-dimethoxybenzene over Ga–MCM-41(M-H)(10) catalyst with different stoichiometric ratio 1,2-DMB/AC

Stoichiometric ratio 1,2-DMB/AC	Time*, min	Selectivity to 3,4-dimethoxyacetophenone, %	Apparent rate constant k_a, 10^3 min^{-1}
1	255.3	100.0	10.1
5	95.0	100.0	40.3
10	64.3	100.0	70.2

Note: A reaction temperature of 333 K, catalyst weight of 0.1 g. * Time required for complete conversion of acetic anhydride.

Table 6. The conversion and the selectivity in the acetylation of 1,2-dimethoxybenzene over Ga–MCM-41(M-H)(10) catalyst with different weight of the catalyst

Weight of the catalyst, g	Time*, min	Selectivity to 3,4-dimethoxyacetophenone, %	Apparent rate constant k_a, 10^3 min^{-1}
0.02	289.5	100.0	8.9
0.1	95.0	100.0	40.3
0.2	58.9	100.0	79.8

Note: A reaction temperature of 333 K, stoichiometric ratio 1,2-DMB/AC = 5.
* Time required for complete conversion of acetic anhydride.

a reaction temperature of 333 K as a function of reaction time and the results are/shown in Table 5. When the 1,2-DMB/AC ratio was varied, the rate of conversion of acetic anhydride was significantly affected. At a reaction temperature of 333 K conversion of acetic anhydride increased when the 1,2-DMB/AC ratio was increased from 1 to 10, while the selectivity to 3,4-dimethoxyacetophenone remained nearly constant in all cases. It appears that at enhanced 1,2-DMB/AC ratios molecules of 1,2-dimethoxybenzene can be adsorbed on the catalysts surface in larger amounts than acetic anhydride.

The effect of the catalyst weight on the acetylation of 1,2-dimethoxybenzene with acetic anhydride. The weight of the catalysts was varied to study its influence on conversion of acetic anhydride in the acetylation of 1,2-dimethoxybenzene over Ga–MCM-41(M-H)(10). CI The weight of the catalysts in the reaction mixture was changed from 0.02 to 0.2 g. Table 6 shows the influence of the weight of the Ga–MCM-41(M-H)(10) catalyst on the rate of conversion of the acetic anhydride in the acetylation of 1,2-dimethoxybenzene. The concentration of the catalyst in the reaction mixture has a huge impact on the apparent reaction rate constant At a reaction temperature of 333 K and the stoichiometric ratio 1,2-DMB/AC = 5 the rate of conversion of the acetic anhydride increased as the catalyst weight was increased from 0.02 to 0.2 g, whereas 100% selectivity to 3,4-dimethoxyacetophenone was maintained. This behaviour can probably be explained by a larger number of active sites on the catalyst surface.

Recycling of the catalysts. The recyclability was investigated in the acetylation of 1,2-DMB over Ga–MCM-41(M-H)(10) at a reaction temperature of 333 K, a reaction time of 2 h, and a 1,2-DMB/AC ratio of 5. After the reaction, the catalyst was filtered, washed several times with acetone and dried in an oven at 393 K. Then, the catalyst was activated at 823 K for 6 h in oxygen. The recyclability tests were carried out two times and the procedure for the activation was repeated every time after the reaction. The results illustrating recyclability of the catalyst are given in Table 7. The catalyst shows approximately similar conversion after two cycles, without any loss selectivity. This shows that the catalyst is very stable under the specified reaction conditions, and can be used in the recycle regime.

Applications to other aromatic compounds. The acetylation of other substrates with acetic anhydride was conducted using the Ga–MCM-41(10) under the optimized reaction conditions. The information of the reaction conditions and the relevant experimental results are presented in Table 8. The catalyst shows a remarkable performance in the acetylation of aromatics. In the case of acetylation of méthoxybenzène (anisole), it was observed that the time required for complete conversion of acetic anhydride over Ga–MCM-41(M-H)(10) catalyst is 27 min with 98.5% selectivity to (*p*) 4-methoxy-

Table 7. Effect of recycling of the catalyst in the acetylation of 1,2-dimethoxybenzene over Ga–MCM-41(M-H) (10)

Catalyst	Time*, min	Selectivity to 3,4-dimethoxyacetophenone, %	Apparent rate constant k_a, 10^3 min^{-1}
Fresh	95.0	100.0	40.3
First reuse	99.2	100.0	37.6
Second reuse	102.5	100.0	33.9

Note: A reaction temperature of 333 K, stoichiometric ratio 1,2-DMB/AC = 5, catalyst weight of 0.1 g.
* Time required for complete conversion of acetic anhydride.

Table 8. Acetylation of different aromatic substrates over Ga–MCM-41(M-H)(10) catalyst at a reaction temperature of 333 K

Substituent	Time*, min	Reaction products (Selectivity, %)
1,2-Dimethoxybenzene	95	3,4-dimethoxyacetophenone (100%)
Methoxybenzene (anisole)	27	***p*-methoxyacetophenone (98.5%) ***o*-methoxyacetophenone (1.5%)
2-Methoxynaphthalene	37	**1-acetyl-2-methoxynaphthalene (97.4%) **6-acetyl-2-methoxynaphthalene (2.6%)

Notes: * Time required for complete conversion of acetic anhydride.
** What does it mean.

acetophenone. The rest is accounted for by (*o*) 2-methoxyacetophenone. Table 8 is also supplemented by the data on the acetylation of 2-methoxynaphthalene with acetic anhydride and nitrobenzene as a solvent. A 97.4% selectivity to 1-acetyl-2-methoxynaphthalene and a selectivity of 2.6% to 6-acetyl-2-methoxynaphthalene were recorded. At a lower reaction temperature the formation of sterically hindered but kinetically favoured product, 1-acetyl-2-methoxynaphthalene, has also been observed in the presence of the zeolite catalysts with an increased external surface area and in the presence of the proton exchanged MCM-41 catalyst. In the reactions over these materials the position 1 seems to be the most activated site [21, 22]. Therefore, the preferential formation of 1-acetyl-2-methoxynaphthalene over the Ga–MCM-41 (M-H) catalyst could be best explained by the fact that this catalytic system has a high surface area, appreciable pore volume, and large pores. All these properties facilitate the formation of the kinetically favoured 1-acetyl-2-methoxynaphthalene instead of the generation of thermodynamically favoured 6-acetyl-2-methoxynaphthalene.

Ordered hexagonal Ga–MCM-41 mesoporous molecular sieves with a high specific surface area were successfully synthesized via microwave irradiation method. After the calcination, the template was effectively removed. The Si/Ga molar ratio is a key factor affecting the textural and structural regularity of Ga–MCM-41 mesoporous molecular sieves. High gallium content is unfavourable to the formation of the Ga–MCM-41 with highly ordered mesoporous structure. These samples have a large number of acid sites with moderate acidity. The study of the liquid phase of acetylation of 1,2-dimethoxybenzene and other two aromatic compounds with acetic anhydride using Ga–MCM-41 solids shows that these catalysts show remarkable activity and can also be repeatedly reused in this reactions.

REFERENCES

1. Laha, S.C., Kamalakar, G., and Glaser, R., *Microporous Mesoporous Mater.*, 2006, vol. 90, p. 45.
2. Bachari, K. and Lamouchi, M., *J. Cluster Sci.*, 2009, vol. 20, p. 573.
3. Jhung, S.H., Chang, J.-S., Hwang, J.S., and Park, S.-E., *Microporous Mesoporous Mater.*, 2003, vol. 64, p. 33.
4. Bachari, K., Guerroudj, R.M., and Lamouchi, M., *React. Kinet. Mech. Catal.*, 2011, vol. 102, p. 219.
5. Tompsett, G., Conner, W.C., and Yngvesson, K.S., *Chem. Phys. Chem.*, 2006, vol. 7, p. 296.
6. Park, S.-E., Chang, J.-S., Hwang, Y.K., Kim, D.S., Jhung, S.H., and Hwang, J.-S., *Catal. Surv. Asia*, 2004, vol. 8, p. 91.
7. Bachari, K. and Lamouchi, M., *Transition Met. Chem.,* 2009, vol. 34, p. 529.
8. Franck, G. and Stadelhofer, G.W., *Industrial Aromatic Chemistry*, Berlin: Springer, 1998.
9. Gore, P.H., in *Friedel–Crafts and Related Reactions*, Olah, G.A., Ed., New York: Wiley-Interscience, 1964, vol. 3, p. 72.

10. Guidotti, M., Canaff, C., Coustard, J.M., Magnoux, P., and Guisnet, M., *J. Catal.*, 2005, vol. 230, p. 375.
11. Bachiller-Baeza, B. and Anderson, J.A., *J. Catal.*, 2004, vol. 228, p. 225.
12. Quaschning, V., Deutsch, J., Druska, P., and Lieske, H.J., *J. Catal.*, 2005, vol. 231, p. 269.
13. Derouane, E.G., Crehan, G., Dillon, C.J., Bethell, D., He, H., and Derouane-Abd Hamid, S.B., *J. Catal.*, 2000, vol. 194, p. 410.
14. Raja, T., Singh, A.P., Ramaswamy, A.V., Finiels, A., and Moreau, P., *Appl. Catal., A*, 2001, vol. 211, p. 31.
15. Kaur, J., Griffin, K., Harrison, B., and Kozhevnikov, I.V., *J. Catal.*, 2002, vol. 208, p. 448.
16. Kozhevnikov, I.V., *Appl. Catal., A*, 2003, vol. 256, p. 3.
17. Cardoso, A.M., Alves, W.,Jr., Gonzaga, A.R.E., Augiar, L.M.G., and Andrade, H.M.C., *J. Mol. Catal. A: Chem.*, 2004, vol. 209, p. 189.
18. Vinu, A., Justus, J., Anand, C., Sawant, D.P., Ariga, K., Mori, T., Srinivasu, P., Balasubramanian, V.V., Velmathi, S., and Alam, S., *Microporous Mesoporous Mater.*, 2008, vol. 116, p. 108.
19. Beck, J.S., Vartuli, J.C., Roth, W.J., Leonowicz, M.E., Kresge, C.T., Schmitt, K.D., Chu, C.T.W., Olson, D.H., Sheppard, E.W., McCullen, S.B., Higgins, J.B., and Schlenker, J.L., *J. Am. Chem. Soc.*, 1992, vol. 114, p. 10834.
20. Chen, L.F., Noreña, L.E., Navarrete, J., and Wang, J.A., *Mater. Chem. Phys.*, 2006, vol. 97, p. 236.
21. Kantam, M.L., Ranganath, K.V.S., Sateesh, M., Kumar, K.B.S., and Choudary, B.M., *J. Mol. Catal. A: Chem.*, 2005, vol. 225, p. 15.
22. Andy, P., Garcia-Martinex, J., Lee, G., Gonzalez, H., Jones, C.W., and Davis, M.E., *J. Catal.*, 2000, vol. 192, p. 215.